International Journal of Biological Macromolecules 67 (2014) 401–408

Contents lists available at ScienceDirect

International Journal of Biological Macromolecules

journal homepage: www.elsevier.com/locate/ijbiomac

Bacterial cellulose and hyaluronic acid hybrid membranes: Production and characterization

Tatyane Duran Lopes[a], Izabel Cristina Riegel-Vidotti[b], Aline Grein[b], Cesar Augusto Tischer[a], Paula Cristina de Sousa Faria-Tischer[a,*]

[a] Department of Biochemistry and Biotechnology, CCE, State University of Londrina, PO Box 6001, 86051-990 Londrina, PR, Brazil
[b] Departamento de Química, Universidade Federal do Paraná (UFPR), CxP 19081, CEP 81531-980 Curitiba, PR, Brazil

ARTICLE INFO

Article history:
Received 2 December 2013
Received in revised form 18 March 2014
Accepted 19 March 2014
Available online 2 April 2014

Keywords:
Bacterial cellulose
Hyaluronic acid
Hybrid membranes
Scaffolds
Properties

ABSTRACT

In this study, the effect of the addition of hyaluronic acid (HA) on bacterial cellulose (BC) production, under static conditions was evaluated in terms of the properties of the resulting BC hybrid membranes. HA was added to the fermentation process in three distinct time points: first day (BC-T0), third day (BC-T3) and sixth day (BC-T6). Analyses of FT-IR and CP/MAS ^{13}C NMR confirmed the presence of HA in bacterial cellulose membranes. The crystal structure, crystallinity index (I_c) surface roughness, thermal stability and hybrophobic/hydrophilic character changed. Membranes with higher roughness were produced with HA added on the first and third day of fermentation process. The surface energy of BC/HA membranes was calculated and more hydrophilic membranes were produced by the addition of HA on the third and sixth day, also resulting in more thermally stable materials. The results demonstrate that bacterial cellulose/hyaluronic acid hybrid membranes can be produced in situ and suggest that HA interacts with the sub-elementary bacterial cellulose fibrils, changing the properties of the membranes. The study and understanding of the factors that affect those properties are of utmost importance for the safe and efficient use of BC as biomaterials in numerous applications, specifically in the biological field.

1. Introduction

One of the main requirements of any biomedical material is that it must be biocompatible, which is the ability to remain in contact with living tissue without causing any toxic or allergic side effects. Because of its unique properties, bacterial cellulose (BC) or microbial cellulose (MC) has been shown to be a highly effective wound dressing material. In fact, the results of various studies indicate that topical applications of BC membranes improve the healing process of burns and chronic wounds [1].

The first use explored of bacterial cellulose was as new skin substitute and membranes of bacterial cellulose commercialized and produced in Brazil as Biofill®, Bionext® and Membracel®, proved to be a very successful wound covering for skin problems such as burns and chronic ulcers [2–6]. Another product called XCell, which is manufactured by Xylos Corporation was very effective in (a) promoting autolytic debridement, (b) reducing pain, and (c) accelerating granulation, all of which are important for proper wound healing [7]. Several research groups in different places of world (United States, Canada, China, Brazil, Portugal, Japan, Sweden, France, Spain, Italy and others) develop researches with this biotechnological product and because of its biofabrication mode, great potential for use in novel materials have emerged.

The first studies with bacterial cellulose started with static fermentation (films production), after BC spheres [8,9] or fiber bundles were produced from agitated conditions (shaking the reactor), hollow tubes were prepared not directly in the reactor vessel but on a glass or silicon cylinder as a matrix/template is placed in the culture medium inside of the reactor [10]. The small and short tubes are useful as blood vessel substitutes in microsurgery; the larger represent novel types of cardiovascular implants [11].

BC hydrogel have recently been produced using porous wax particles in the fermentation broth, leading to macroporous BC materials that can be used to support human smooth muscle cell migration, proliferation, and differentiation [12]. These BC materials are very attractive for use as a scaffold for regeneration of cartilage, bone, urethra, and bladder [11]. Scaffolds are mechanical substrates that may interact with the cells and the surrounding tissue [13]; they can be classified depending on their morphology as hydrogels, fibrous constructs and porous scaffolds [14].

* Corresponding author. Tel.: +55 4399370085.
E-mail addresses: izabel.riegel@ufpr.br (I.C. Riegel-Vidotti), cesar.tischer@uel.br (C.A. Tischer), paula.tischer@pq.cnpq.br, paula.tischer@gmail.com (P.C.d.S. Faria-Tischer).

http://dx.doi.org/10.1016/j.ijbiomac.2014.03.047
0141-8130/

Different additives were added to *Acetobacter xylinum*, nowadays *Gluconoacetobacter xylinum*, growth media for study their influence on yield, morphology and crystalline constituents of BC, including agar [15], sodium alginate [16], carboxymethylcellulose (CMC) [17,18], pectin [16], carbon nanotubes [19], polyacrylamide [20], xylan [21], xyloglucan [22], acetyl glucomannan [23], lignosulfonate [24] and microcrystalline cellulose [25].

The fabrication of scaffolds from natural materials, such as hyaluronic acid (HA), can impart intrinsic signals within the structure that can enhance tissue formation. HA is a linear polysaccharide formed from disaccharide units containing *N*-acetyl-D-glucosamine and glucuronic acid and is a common component of synovial fluid (SF) and extracellular matrix (ECM). Industry has turned to microbial fermentation processes for the production of HA; *Streptococcus epizooticus* and *Streptococcus equi* strains are commercially used in HA synthesis [26]. *Bacillus subtilis*, carrying the *hasA* gene from *Streptococcus equisimilis* encoding the enzyme HA synthase is one of the promising potential candidates for production on a large scale [27].

Ocular surgery, visco supplementation for osteoarthritis, in cosmetics, in ophthalmology, in aesthetic medicine, in surgery, topical drug delivery, wound healing and in tissue engineering are some of HA uses [28–30]. However, the poor mechanical properties, rapid degradation and clearance in vivo of uncrosslinked soluble HA limit many direct clinical applications.

Therefore, the objectives of this study were to observe if HA can be introduced in the bacterial cellulose membranes during fermentation process and analyze the interference with in situ BC crystallization, morphology, thermal stability and surface properties.

Investigations have reported the synthesis of novel biomimetic hydrogels based on crosslinking cellulose derivatives with hyaluronic acid, between hydroxyethylcellulose (HEC) and carboxymethylcellulose (CMCNa) through the difunctional crosslinker divinyl sulfone [31] or with a water-soluble carbodiimide [32]. These methods are important and show potential for development of biomimetic products but they are complex, expensive and the biocompatibility of the crosslinking agent used is particularly important.

In our work we evaluated the production of hybrid membranes through a simple, fast and low-cost method, without addition of any component biologically incompatible, seeking the formation of hybrid membranes with different crystallinity, morphology, roughness of surface and with distinct surface properties, which can make them useful as future scaffold for tissue regeneration.

2. Materials and methods

2.1. Materials

The bacterial strain used in this study was *A. xylinum* ATCC 23769 (reclassified as the genus *Gluconacetobacter*) obtained from Foundation André Tosello from Campinas, São Paulo which was grown in a glucose medium based on the Hestrin–Schramm's medium culture [33], this glucose medium is composed of 4 g L^{-1} glucose, 5 g L^{-1} yeast extract, 5 g L^{-1} peptone, 2.7 g L^{-1} Na_2HPO_4, and 1.15 g L^{-1} citric acid. All media were autoclaved at 121 °C and 1.02 atm for 20 min. The hyaluronic acid (sodium hyaluronate) from *S. equi* (53747) (CAS number 9067-32-7) was added in the fermentation process.

2.2. Methods

2.2.1. Storage of bacteria and growth conditions

The cell suspensions of *G. xylinum* were stored at −80 °C in glycerol solution. One milliliter of cell suspension stored at −80 °C was added into flask with 40 mL of Hestrin–Schramm's medium. The pre-inoculum was prepared by growing *G. xylinum* at 28 °C using a rotary shaker (180 rpm) for two days.

2.2.2. Fermentation process

During growth in shake flasks the culture appeared as a fine suspension of cells and irregular clumps of different sizes. The volume of inoculum was 10% of the total volume, to the static process. After two days of growth the ratio of clumps to cell suspension was transferred to a 160 mL flask containing Hestrin–Schramm's medium. The static fermentation process was realized at 28 °C during 10 days. At the end of this period the bacterial cellulose membranes were removed from static culture and purified by immersion in an aqueous solution of 0.1 mol L^{-1} NaOH for one day. The BC pellicles were then washed with deionized water several times to completely remove the alkali. The membranes were dried in stove at 40 °C.

2.2.3. Bacterial cellulose/hyaluronic acid membranes production

For the production of hybrid membranes, hyaluronic acid (sodium hyaluronate, $M_W = 1.1–1.7 \times 10^6$ Da, predispersed in water 1%) was added to the fermentation process at different time points: first day of fermentation (T0), which corresponds to the moment of *G. xylinum* inoculation, third day (T3) and sixth day (T6) after the start of fermentation. The modified membranes were identified, respectively as BC-T0, BC-T3 and BC-T6. To eliminate impurities such as bacteria and other interfering substances, cellulose membrane floating on the surface of the culture medium was collected and immersed in an aqueous solution of 0.1 mol L^{-1} NaOH for one day. The BC pellicles were then washed with deionized water several times to completely remove the alkali, and afterwards dried in stove at 40 °C (same procedure described above).

2.2.4. Characterization of membranes native and modified

2.2.4.1. X-ray diffraction—XRD. X-ray diffraction spectra of the bacterial cellulose membranes were obtained using a Panalytical X'Pert PRO MPD diffractometer (The Netherlands), using *K*α copper radiation (λ = 1.5418 Å), at 40 kV and 30 mA. All assays were performed with ramping at 1° min^{-1}, analyzing the range of 5–40° (2θ).

The degree of crystallinity was taken as $CrI = (I_{200} - I_{am})/I_{200}$, where I_{200} is the overall intensity of the peak at 2θ (about 22.9°) and I_{am} is the intensity of the baseline at 2θ (about 18°) [34].

2.2.4.2. Fourier transform infrared spectroscopy analysis–FT-IR. FT-IR spectra of dried membranes were recorded on a FT-IR Bommen MB-100 in transmission mode in the range of 4000–400 cm^{-1} at a resolution of 4 cm^{-1}.

2.2.4.3. Solid-state CP-MAS ^{13}C NMR. NMR experiments were performed at 24 °C using a ADVANCE 400 (Bruker Spectrometer) operated at a ^{13}C frequency of 100.6 MHz, using the technique of cross-polarization (CP) at the magic angle (MAS) from finely comminuted or particulate samples and using glycine as external standard.

2.2.4.4. Scanning electron microscopy—SEM. The qualitative assessment of the morphology of the membranes was performed using a FEI Quanta 200 microscope (Oregon, USA). Membranes pieces were mounted on the bronze stubs using double-sided tape and then coated with a layer of gold (40–50 nm), allowing surface visualization. The average width of the microfibrils was estimated from measures performed on 10 microfibrils, using the software ImageJ.

2.2.4.5. Atomic force microscopy—AFM. Tapping mode AFM images were recorded in air using a Agilent 550 microscope (Agilent

Technologies, Santa Clara, CA, USA) at room temperature (~24 °C). Height mode images ($6 \times 6\,\mu m^2$ and 512×512 pixel^2) were collected with a scan speed between 1 and 3 Hz. The operating point was adjusted to minimize the interaction between the tip and sample to avoid layer deformation. Image treatment was performed using Gwyddion software and the topography and the roughness were analyzed of the native and modified films. The RMS roughness (Rq) of the membranes, defined as the standard deviation of the elevation z-values, within the given area, was determined [35].

2.2.4.6. Thermal gravimetric analysis (TG). Thermogravimetric analysis (TG) of native and hybrid bacterial cellulose membranes were carried out under air atmosphere with a heating rate of 30 °C per min in the temperature range from 25 to 600 °C, using a TGA 50, Shimadzu.

2.2.4.7. Surface energy. The surface energy (SE) of BC/HA membranes were calculated by the sessile drop method. It measured the contact angle (θ) of uniform drops (8 μL) of ultrapure water ($\gamma_L = 72.8$ mN m^{-1}) deposited onto the membranes. A DataPhysics GmbH (Filderstadt, Germany) tensiometer, model OCA 15 plus was used. Measurements were performed at 24 °C using a 500 μL syringe (Hamilton). The considered values of θ represent the average of at least 10 measurements on each membrane.

The Neumann equation [36] was employed to calculate the SE of each membrane, where γ_S is the surface energy of the membrane (mN m^{-1}), γ_L is the surface tension of the test liquid and β was taken as 0.0001247 (m^2 mN^{-1} m)^2. By this method, only one test liquid is required to calculate the SE.

$$\cos\theta = -1 + 2\sqrt{\frac{\gamma_S}{\gamma_L}}e^{-\beta(\gamma_L-\gamma_S)^2} \quad (1)$$

The calculations were performed by means of the ACS20 software from DataPhysics (Filderstadt, Germany).

3. Results

3.1. Crystallinity and structural aspects of native and hybrid bacterial cellulose/hyaluronic acid membranes

The XRD profile of a native BC and BC/hyaluronic acid membranes shown in Fig. 1 corresponds to profile of cellulose I, with reflections at 14.6°, 16.9° and 22.8° indexed as 1 0 0, 0 1 0 and 1 1 0, respectively in the triclinic unit cell of allomorph Iα [37]. The low relative intensity of the 1 0 0 reflection reveals a strong uniplanarity of the cellulose ribbons in the dry film mainly in native BC and in BC-T0 membranes. The XRD profile of membranes produced in the presence of hyaluronic acid was similar to native BC within the same angular domain, the addition of hyaluronic acid after the starting of bacterial cellulose synthesis seems to reduce the uniplanarity of the ribbons in the dried films (Fig. 1b and c).

The crystallinity of the membranes varied according to the point in time when hyaluronic acid was added to the fermentation process. The degree of crystallinity of BC membrane biosynthesized in the absence of HA (BC) and that produced with HA added in the first day of fermentation (BC-T0) presented similar crystallinity. The membranes produced with the addition of HA on the third and sixth day after the start of fermentation process showed higher crystallinity (Table 1).

The presence of hyaluronic acid in the bacterial cellulose membranes was proved by FT-IR. This technique is sensitive to the hydrogen-bonding patterns that provide cohesion to the chain packing. The predominance of Iα was observed and confirmed in the FT-IR spectra from the OH-stretching region, as shown in Fig. 2, where an Iα-specific band was exclusively observed at 3240 cm^{-1}.

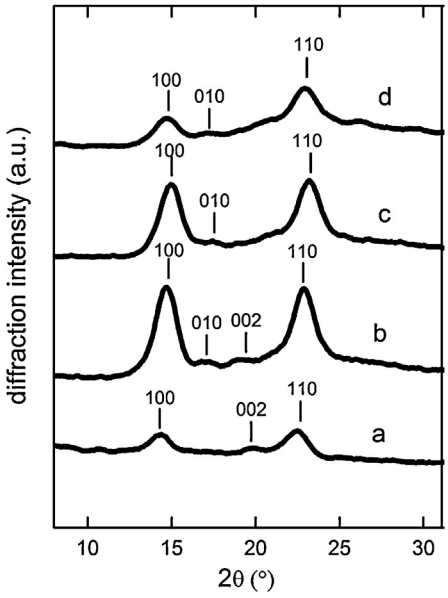

Fig. 1. Ray-X diffractions profiles of BC-T0 (a), BC-T3 (b), BC-T6 (c) and native BC (d) films. The indexation of native BC corresponds to that of allomorph Iα.

Although they differ in crystallinity, all of them exhibit typical features of crystalline cellulose, such as strong transmission of OH stretching vibrations in the range of 3600–3000 cm^{-1}, CH and CH_2 stretching vibrations in the range of 3000–2800 cm^{-1}, and typically C—O and C—C stretching motion in the range of 1200–900 cm^{-1}, fingerprint [38]. It has been observed that two peaks around 750 and 710 cm^{-1} are characteristic for Iα and Iβ allomorphs, respectively [39].

The spectrum of hyaluronic acid (Fig. 2a) shows the strong band at about 3412 cm^{-1} which is rather broad and can be assigned to hydrogen-bonded O—H and N—H stretching vibrations. A group of overlapping bands of moderate intensity is observed around 2916 cm^{-1} which are due to the C—H stretching vibrations. The bands at 1617 and 1411 cm^{-1} can be attributed to the asymmetric (C—O) and symmetric (C—O) stretching modes of the planar carboxyl groups in the hyaluronate [40]. The absorption bands at about 1653, 1563 and 1320 cm^{-1} are characteristic of the amide I, II, and III band, respectively [41].

In order to get more information on carboxylate groups Haxaire et al. [42] compared the spectrum of hyaluronic acid with that of a dried hyaluronic acid film (Na^+ replaced by H^+) that identified the carboxyl $\upsilon_{C=O}$ band as a band at 1745 cm^{-1} and the υ_{C-O} band of the same COOH with a maximum at 1220 cm^{-1}. The band at 1745 cm^{-1} is not present in hyaluronic acid (Fig. 2a) once it appears clearly in the hybrid films (Fig. 2c–e), evidencing that the HA is in the sodium form whereas the HA/hybrid membrane is protonated. This difference would be derived from specified interaction between the hydroxyl group of cellulose and carboxyl group of HA during fermentation process.

The presence of hyaluronic acid was also determined by ^{13}C CP MAS NMR. The spectrum of the hyaluronic acid shows centered at 101.6 ppm both anomeric carbons of the glucuronic acid and the *N*-acetyl glucosamine. The methyl from *N*-acetyl group can be observed at 23.3 ppm with the C2 linked to N at 55.6 ppm (Fig. 3a). The carbonyl carbons from carboxylic acid and acetyl are overlapped at 175 ppm. The NMR spectrum of the BC-T0 sample (Fig. 3b) shows mainly signals that correspond to the bacterial cellulose with a crystallinity of 61%, measured from C4 integration. Note that the usual crystallinity was not changed greatly in comparison with native BC (Table 1).

Table 1
Crystallinity index (I_c) calculated from XRD profiles and CP-MAS NMR, acid content calculated from CP-MAS NMR (integration of carboxilic and carbonil groups against the anomeric signals), width of ribbons and roughness (RMS, measured on $6 \times 6\ \mu m^2$), of native and hybrid membranes.

Sample	I_c XRD (%)	I_c CP MAS NMR (%)	Acid content CP MAS NMR (%)	Average ribbon width (nm) [range (nm)]	RMS (nm)
BC	62	64	–	100 [70–140]	21.6
BC-T0	60	61	82	124 [90–150]	49.5
BC-T3	68	70	48	74 [70–90]	39.3
BC-T6	66	66	50	105 [50–150]	14.2

Signals from HA can be seen, the methyl group of the acetyl is present at ~23 ppm the C2 of the *N*-acetyl also at ~55 ppm, as well as the carbonyl carbon at ~174 ppm. Some new signals are observed at the spectrum that could be attributed to peptides or proteins, at 30 ppm, 33 ppm and 41 ppm for CH_2, also at 130 ppm for aromatic rings, and eventually overlapped at 174 ppm.

The BC-T3 spectrum evidences a BC with crystallinity of 70%, with the presence of the same signals ascribed to HA, and to the presence of proteins, both in minor quantity. Lower intensity of these signals is seen on BC-T6 sample, with a decrease to 66% of crystallinity.

Acid content in each membrane (relative to the integration of carboxylic and carbonyl groups against the anomeric signals; $HA_{content} = I_{acid}/(I_{anomeric} \times 100\%)$ is demonstrated in Table 1, showing the high different percentage of hyaluronic acid content in function of the its time of exposure to *G. xylinum* in the fermentation process.

Besides the presence of unexpected signals at 20–50 ppm, the HA acetyl (~23 ppm) and *N*-acetyl (~55 ppm) can be distinguished and assigned on the spectrum, as well as the C2 to C5 contribution between 70 and 80 ppm disturbing the usual cellulose spectrum, that can be also observed at BC-T3 and BC-T6.

The presence of peptides is usual attached to hyaluronic acid; the RGD sequence Arg–Gly–Asp [43] as a tripeptide or variations of these in linear extension [44] or as cyclic structures that play an important role on cell adhesion [45,46]. The presence of signals found on NMR spectrum, mainly BC-T0, agree with those observed by Asakura and colleagues [47] that attributed methyl, Cα and Cβ signals for Arg, Gly and Asp in the same region between 15 and 50 ppm.

3.2. Surface physical properties of BC/HA hybrid membranes determined by SEM, AFM and contact angle measurements

The SEM micrographs of native BC and hybrid membranes are shown in Fig. 4. At the observed length scale, no significant differences between the membranes surfaces were evidenced, since all exhibit a mesh-like morphology. Therefore, the general appearance of cellulose membranes surface was not intensely affected by the inclusion of HA in the medium. Fig. 4a shows the reticulated structure of the cellulose, which is the typical expected structure for cellulose produced by *G. xylinum* in static fermentation. In all images the ribbons are randomly oriented originating a well-interconnected network structure with the presence of small pores.

In regard to the surface of BC-T6 membrane (Fig. 4d) it can be identified by the deposition of a material that most probably corresponds to the hyaluronic acid added to the fermentation process.

The average width of ribbons was measured for all membranes. Native BC and BC-T6 hybrid membrane presented very close values, i.e., 100 nm and 105 nm, respectively. In different way, the addition of hyaluronic acid at the fermentation start (BC-T0) seems to increase the width of the ribbons (Table 1).

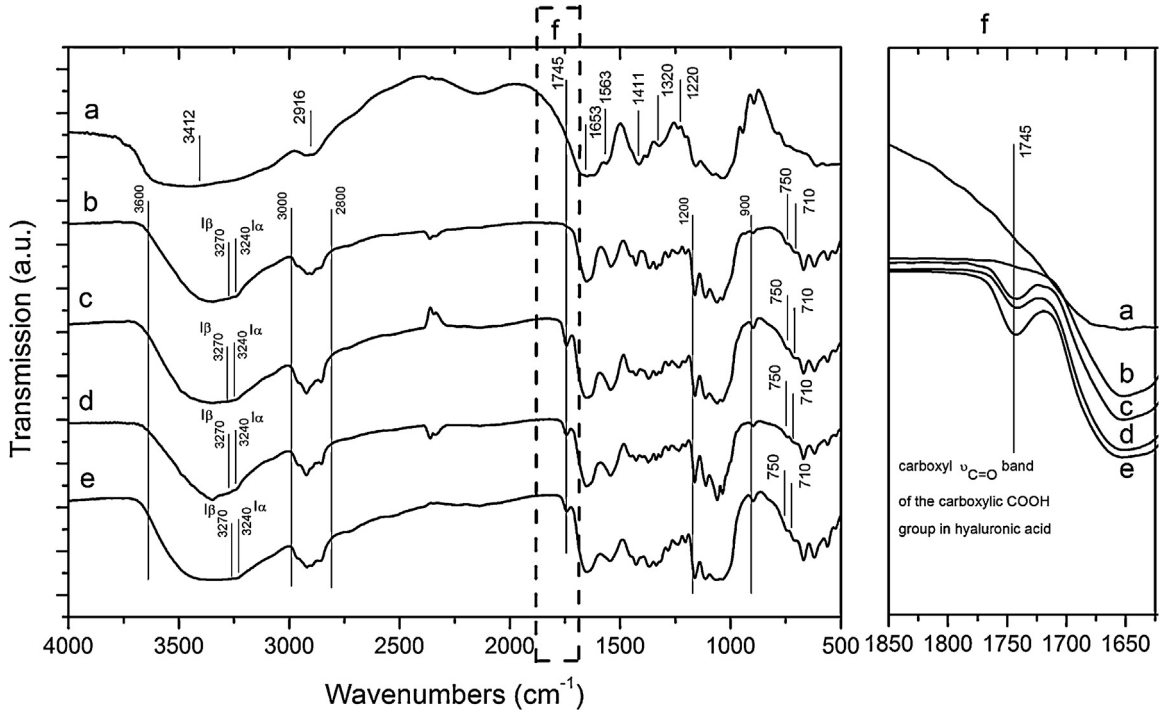

Fig. 2. FTIR spectra of samples (a) hyaluronic acid (HA), (b) native bacterial cellulose (BC), (c) BC-T0, (d) BC-T3, (e) BC-T6. The band of 1745 cm^{-1} is shown in box (f).

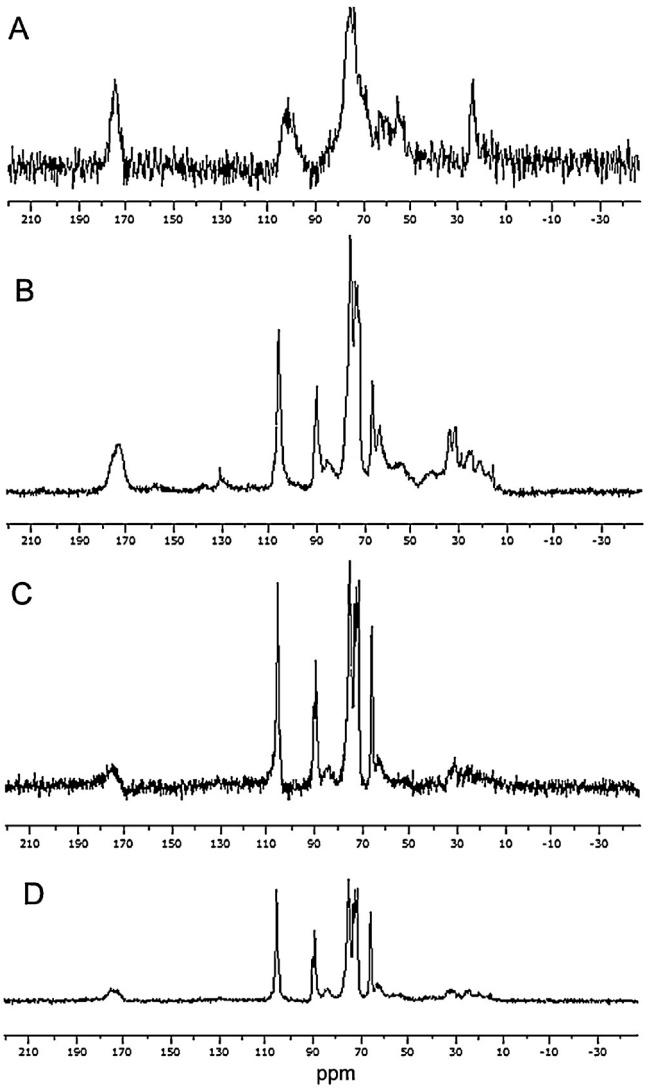

Fig. 3. Solid state ^{13}C CP MAS NMR spectra of the hyaluronic acid (a), BC-T0 (b), BC-T3 (c) and BC-T6 (d).

The surface features of native and modified membranes also were examined through atomic force microscopy (AFM) in order to access more details about the surface morphology of the membranes and the effect of HA. The comparison of the AFM images of native and hybrid membranes reveals a change in surface texture with the inclusion of HA. In native bacterial cellulose membrane ribbon bundles are observed (Fig. 5a) and after addition of HA the fibrils are adhered to each other, possibly by means of the incorporation of HA between them.

Table 2
Contact angle of water onto the different hybrid membranes. Surface energies (SE) were calculated according to the Neumann equation.

Sample	θ (°)	SE (mN m^{-1})
BC	36.9 ± 4.0	60.95 ± 0.67
BC-T0	59.6 ± 4.1	48.52 ± 0.77
BC-T3	38.9 ± 4.1	59.47 ± 0.86
BC-T6	29.6 ± 5	64.45 ± 0.85

The surface roughness changed with the presence of HA as function of the moment of its addition. Native BC and BC-T6 show smoother surface morphology with roughness of 21.6 nm and 14.2 nm, respectively (Fig. 5 and Table 1). The addition of HA at the start and on the third day of fermentation process allowed better incorporation of HA between the microfibrils originating rougher surfaces. On the contrary, once the ribbons network is relatively well formed, the HA added to the fermentation culture probably adsorbs onto the ribbons surfaces, promoting the aggregation between the microfibrils and occupation of the membrane pores, resulting in a smoother surface.

Wetting experiments were carried out using water as test liquid to get information on the surface roughness and hydrophobic/hydrophilic character of the membranes. The results are shown in Table 2. The contact angle varied according to the time of the addition of HA to the fermentation process. The lower contact angle was found for BC-T6 and the highest for BC-T0. According to the Neumann equation (Eq. (1)), that employs the cosθ to calculate the surface free energy, the higher is θ, the lower is cosθ, and therefore the surface energy. Low surface energy values correspond to surfaces with high phobic character [48] Therefore, the addition of HA on the sixth day after the start of the fermentation process resulted in surfaces with the more hydrophilic (polar) character. As will be further discussed, and in accordance to the SEM and AFM results, in BC-T6 the HA molecules seem to be adsorbed onto BC fibrils, resulting in a smoother and more hydrophilic surface.

We believe that the HA added on the first day of the fermentation processes renders trapped inside the membrane. Therefore, during the course of the fermentation (up to the 10th day), the free hydroxyl groups of the newly formed BC fibrils (the ones not participating in the intermolecular BC interaction), orientate toward the HA, becoming no longer available to occupy the surface, and lowering the surface hydrophilicity of the material. As an opposing behavior, a highly hydrophilic membrane is obtained when HA is added on the sixth day of fermentation (BC-T6). In this case, the HA adsorbs to the outer BC fibrils, since it is added when they are reasonably well formed. However, we must emphasize that compared to many others biological surfaces, all of the produced membranes are hydrophilic, as seen by the water contact angles ($30° \leq \theta \geq 60°$).

3.3. Thermal gravimetric analysis

The membranes behave distinctly regarding their mass loss as a function of the temperature, according to the time of the addition

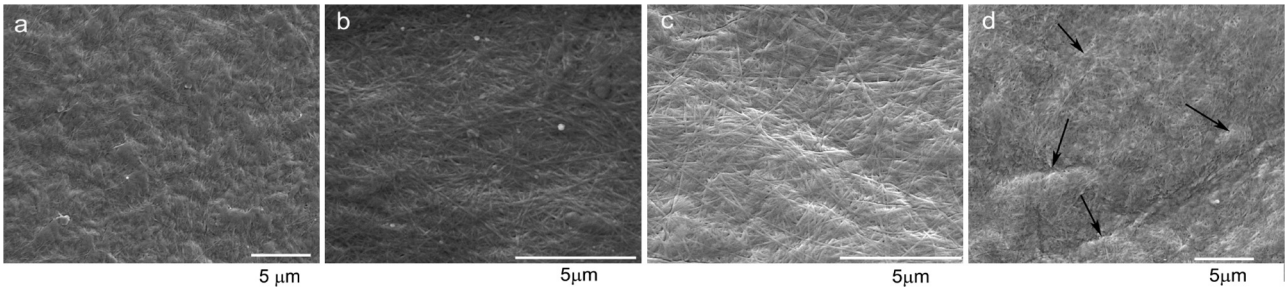

Fig. 4. SEM images of (a) native bacterial cellulose (BC), (b) BC-T0, (c) BC-T3, (d) BC-T6. The arrows show the locals with material deposition.

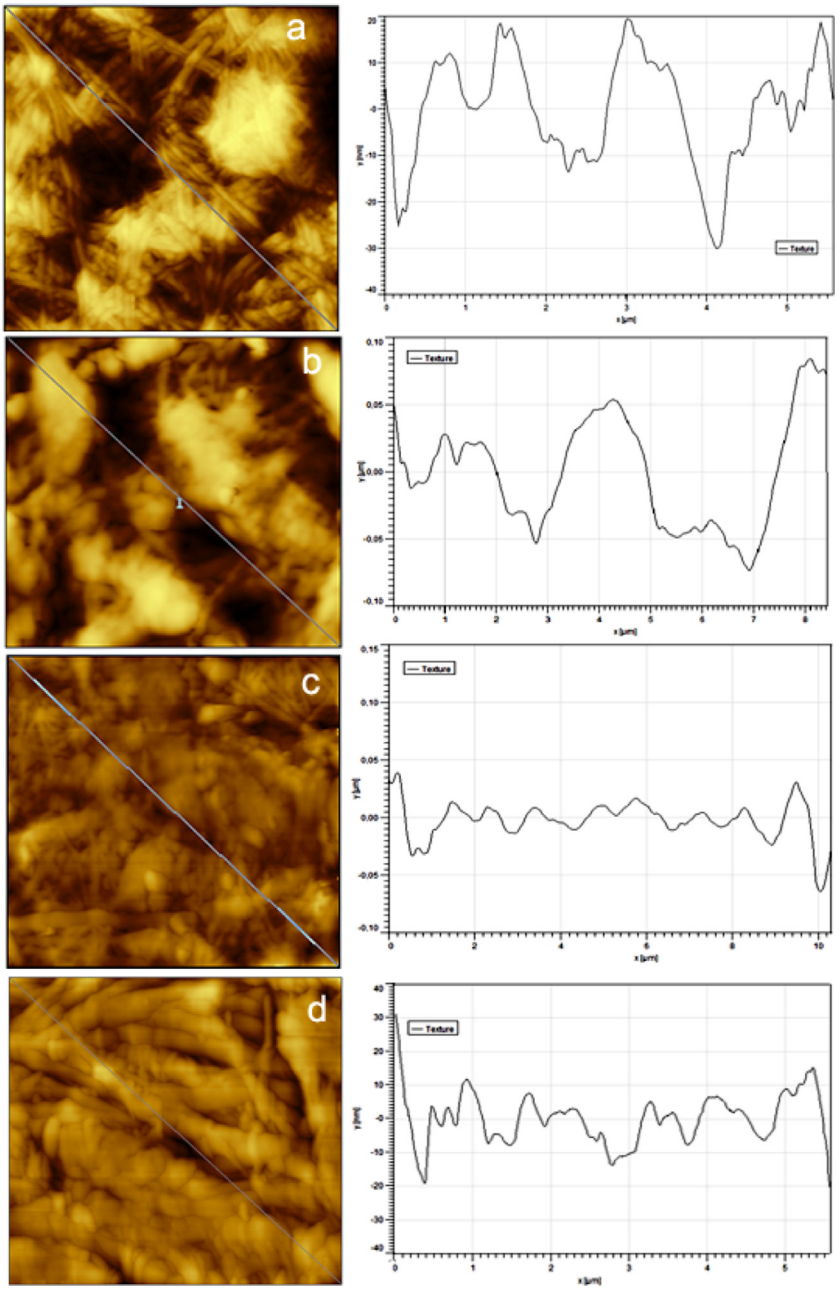

Fig. 5. AFM topography images of (a) native bacterial cellulose (BC), (b) BC-T0, (c) BC-T3, (d) BC-T6. In all samples ($6 \times 6\ \mu m^2$) the texture profile was plotted along the line from top to bottom.

of HA in the fermentation process. The mass loss of all investigated materials occurred in one step as can be observed in Fig. 6. The main mass loss percentage was observed in the temperature range from 150 to 450 °C. The data are displayed in Table 3. From the point of view of the starting of the degradation process, the hybrid membranes are more thermally stable than native BC, as demonstrated by the temperatures T_{onset} (starting of thermal decomposition). However, the temperature where 5% of the mass is lost ($T_{5\%}$) is higher for BC when compared to the hybrid membranes. The loss of mass at lower temperatures (remarkably lower for BC-T3 and BC-T6) can be associated to the availability of HA molecules at the surface of the membranes which would be more readily susceptible to the thermal degradation.

Table 3
Thermogravimetric analysis results (dry basis). $T_{5\%}$ is the temperature corresponding to 5% of mass loss, T_{onset} is the onset temperature of the pyrolysis and T_{max} is the temperature of the maximum weight loss rate.

	BC	BC-T0	BC-T3	BC-T6
Mass loss (%) (150–500 °C)	64.3	61.9	56.6	59.7
T_{onset}	226.4	282.3	292.2	299.3
$T_{5\%}$ (°C)	269.1	246.3	237.9	229.9
T_{max} (°C)	367.0	357.0	356.0	354.1
Residue at 600 °C (%)	32.1	34.0	39.6	37.0

4. Discussion

The biological functions of cellulose are based on its distinct fiber morphology, crystallinity and surface properties. Therefore, the study and understanding of the factors that affect those

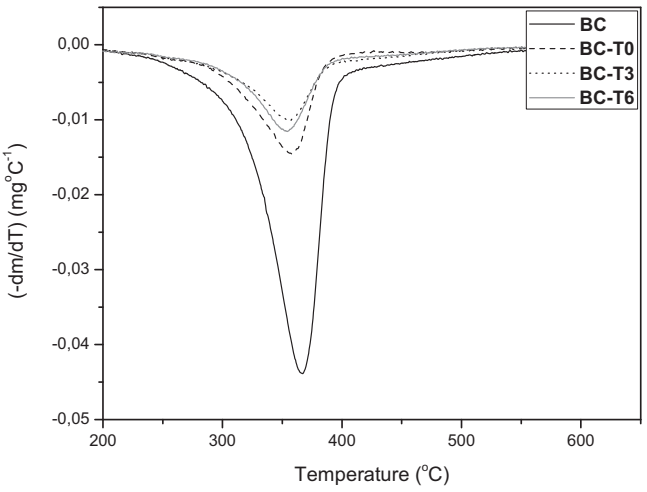

Fig. 6. DTG curves of native bacterial cellulose (BC), BC-T0, BC-T3 and BC-T6 membranes.

properties are of utmost importance for the safe and efficient use of BC as biomaterials.

The biosynthesis of BC involves polymerization and crystallization processes [49] although crystallization occurs as soon as the glucan chains are extruded from the cell, it does not occur instantaneously. Based on the two-step model proposed by Cousins and Brown [48] it was assumed that the factors that affect either step will influence the final structure of the BC. There are several polymorphs of crystalline cellulose (I, II, III, IV). Cellulose I has two polymorphs, a triclinic structure (Iα) and a monoclinic structure (Iβ), which coexist in various proportions depending on the cellulose source [50,51]. In bacterial cellulose the Iα structure is the dominate polymorph [52]. The lattice structures (unit-cell parameters) of Iα and Iβ unit cell are different but despite the differences between these allomorphs, the shifts in the cellulose chain arrangement are small when viewed along the chain axis [43]. It has been shown previously the decrease of bacterial cellulose crystallinity with the increase of carboxymethylcellulose (CMC) concentration (0.2–0.8%) in the medium under agitated fermentation conditions [25]. The impact of CMC was much lower when compared to the addition of sodium alginate (0.04%) for which the crystallinity reduction was from 78 to 59%. [53] The authors suggest that the reduction of crystallinity can be probably due to the shear force stress in an agitated bioreactor. In the presence of water-soluble hemicellulose [54], xyloglucan [39,55] and glucomannan [23], it was found that the proportion of cellulose Iα/Iβ decreases. The results revealed that these additives may delay the aggregation of cellulose microfibrils and prohibit the crystallization of cellulose microfibrils, decreasing the crystallite size, crystallinity index and cellulose Iα content.

In different ways of other water soluble polysaccharides, in our study, the addition of HA during the polymerization and crystallization process (on the third and sixth day of fermentation) resulted in an increase of the crystallographic plane 1 1 0 and higher crystallinity index, demonstrating that HA decrease the uniplanarity of cellulose fibrils in the surface membrane and affect also the crystallization process. Therefore, it can be safely concluded that adding HA into the culture medium affects the assembly and crystallization of glucan chains, mainly when HA is added at the start of the fermentation process.

The produced hybrid membranes presented some differences in the width of the ribbons as showed by SEM and AFM. The production of BC follows a hierarchical structure formation that begins with the subelementar fibrils (1.5 nm), aggregation to form microfibrils (3–9 nm in width), and the resulting microfibrils further aggregate to produce a typical ribbon assembly with lateral width near 100 nm [18]. In the previously mentioned study [25] it was observed that the addition of different concentrations of CMC (0.2–1.0%) in the fermentation process slightly decreased the width of cellulose fibrils. Accordingly, our work revealed similar differences in the surface structures as demonstrated in the SEM micrographs.

Apparently the hyaluronic acid can be incorporated into the fibrils during fermentation process increasing the membrane roughness. After six days the membrane was already biosynthesized and probably the HA is present mainly at the surface not between the fibrils, resulting in the surfaces being less rough. These data indicate that there is a change in the rearrangement of BC fibrils in the presence of HA. The CP MAS ^{13}C NMR spectra agree with FT-IR analysis demonstrating that hyaluronic acid was incorporated in the bacterial cellulose produced, also corroborated by NMR, showing 82% of carboxylic acid presence in BC-T0. This can be put in discussion once amide signals appear at ~20–30 ppm (Fig. 3b) suggesting the presence of peptides that contribute to increase the area of the signal at ~174 ppm. The presence of peptides in the hybrid membranes is expected due to the presence of charges on HA.

It is well reported in the literature that the higher the polymer crystallinity, the higher will be its thermal stability. The hybrid membranes are more thermally stable, as mentioned earlier. This result is in accordance to the crystallinity index, calculated from the XRD profiles (Table 1). At the same time, the more stable membranes (higher crystallinity) are more readily prone to lose 5% of their mass. This can be rationalized by the fact that BC-T3 and BC-T6 have more hydrophilic surfaces, most probably due to the presence of HA molecules at the surface that adsorb water very well.

FT-IR analysis revealed evidences of intermolecular interactions between BC and HA via OH/NH groups. Therefore, the carboxylic terminals of the HA would be available at the air interface, increasing the surface energy and the hydrophilic character of the membranes. At the beginning of the fermentation process, the pH is around 3 to 4, which is near the p*K*a of the carboxylic acid moieties. As the BC is produced, the medium pH decreases. When the HA is added under those conditions (third and sixth day after the start of the fermentation) the carboxylic groups would be mainly in their non ionized form allowing the interactions with the formed BC fibrils to occur via NH groups. Therefore, the carboxylic groups will orientate toward the membrane surface.

The HA is trapped on the cellulose network by chain interdiffusion which can promote the formation of a sufficiently stable adhesive interface once anionic polymers are able to develop strong hydrogen bonding; like the interaction of HA and CMC [56] these interactions need to be accompanied by chains interpenetration. The BC-T0 cellulose fibrils grew through the HA, a bulky polymer that may have been folded by the nascent bacterial cellulose, trapping it inside film layers. This explains the lower hydrophilicity of membrane BC-T0 when compared with other hybrid membrane surfaces (Table 3). The HA input on the 3rd and 6th days finds a cellulose membrane formed, and taking into account the production is from surface of liquid to the bottom considering that the *G. xylinum* is an aerobic bacteria, the HA is incorporated at the surface of the membrane, giving rise to more hydrophilic surfaces.

The crystallinity, morphology, surface roughness and surface properties of membranes changed with the presence of HA. The behavior of cells on different materials are dependent on the physiological environment of the cell type used. Proliferation of cells is expected to be higher on surfaces with adequate hydrophilic or hydrophobic character depending on characteristic of its tissue in body. Also it is expected that cells either proliferate or produce extracellular matrix [57]. Previous studies showed the more

hydrophilic surface of material films is the much more cell adhesion on the surface [58,59].

We believe that these new hybrid membranes can be useful for future application in tissue regeneration as scaffold, as temporary supporting structure for growing cells and tissues, once microfibrils of cellulose can provide the structure for cell adhesion whereas the hyaluronic acid contributed to the improvement of the proliferation, migration and differentiation of cells which leads to the formation of specific tissues [60].

5. Conclusions

Hybrid bacterial cellulose/hyaluronic acid membranes were produced in situ, through addition of HA in the fermentation process. The time point of the addition of HA to the fermentation process influences the main properties of BC membrane. Membranes with distinct characteristics were produced through addition of HA at the start of fermentation process (BC-T0) and after the bacterial films have already been synthesized (BC-T3 and BC-T6). When compared to native BC, more hydrophobic (BC-T0) and more hydrophilic (BC-T6) membranes were produced, corresponding also to the rougher and smoother surfaces, respectively. The crystallinity of the film does not seem to be affected by the addition of HA at the start of the fermentation, as well as the uniplanarity, but the addition of HA after the start of fermentation produces films with higher crystallinity and thermal stability.

Acknowledgments

The authors wish to thank the Laboratory of Microscopy and Microanalysis (LMEM), Laboratory of X-Ray Diffraction (LDRX)—Universidade Estadual de Londrina (UEL) for the analyses. Also, many thanks to Prof. Maria Rita Sierakowski for the AFM facilities and tensiometry tests. Conselho Nacional de Desenvolvimento Científico e Tecnológico (CNPq/Brazil) (grant 476453-2010-0) and Rede Nanoglicobiotec/CAPES-Brazil (grant 564741/2010-8) are acknowledged for financial support.

References

[1] W. Czaja, A. Krystynowicz, S. Bielecki, R.M. Brown Jr., Biomaterials 27 (2006) 145–151.
[2] J.D. Fontana, A.M. De Sousa, C.K. Fontana, I.L. Torriani, J.C. Moreschi, B.J. Gallotti, S.J. De Sousa, G.P. Narcisco, J.A. Bichara, L.F. Farah, Appl. Biochem. Biotechnol. 24/25 (1990) 253–264.
[3] D.C.S. Pinto, R.L. Sakai, F.S. Rocha, M.H. Campos, A.A. Souza, C.A. Mattar, P.C.C. Almeida, P.C. Andrade, R. Reis, L. Faiwichow, Rev. Bras. Queimaduras 9 (2010) 155–215.
[4] R.S. Peixoto, D.L.N. Santos, Rev. Bras. Cirurgia Cardiovasc. 78 (1998) 141–145.
[5] C. Rebello, D.A. Almeida, E.M. Lima Jr., M.P. Dornelas, Rev. Bras. Cirurgia Cardiovasc. 77 (1987) 407–414.
[6] J.C. Vieira, A.Z.D. Badin, L.H.A. Calomeno, V. Teixeira, E. Ottoboni, M. Bailak Jr., G. Salles, Arq. Catar. Med. 36 (2007) 94–97.
[7] O. Alvarez, M. Patel, J. Booker, L. Markowitz, Wounds 16 (2004) 224–233.
[8] F.D.E. Goelzer, P.C.S. Faria-Tischer, J.C. Vitorino, M-R. Sierakowski, C.A. Tischer, Mater. Sci. Eng., C 29 (2009) 546–551.
[9] W. Czaja, D. Romanovicz, R.M. Brown, Cellulose 11 (2004) 403–411.
[10] A. Bodin, H. Bäckdahl, H. Fink, L. Gustafsson, B. Risberg, P. Gatenholm, Bioeng. Biotechnol. 97 (2007) 425–434.
[11] P. Gatenholm, D. Klemm, MRS Bull. 35 (2010) 208–213.
[12] H. Bäckdahl, M. Esguerra, D. Delbro, B. Risberg, P. Gatenholm, J. Tissue Eng. Regener. Med. 2 (2008) 320–330.
[13] L. Lu, X. Zhu, R.G. Valenzuela, B.L. Currier, M.J. Yaszemski, Clin. Orthop. Relat. Res. 391 (2001) S251–S270.
[14] J. Raghunath, J. Rollo, K.M. Sales, P.E. Butler, A.M. Seifalian, Biotechnol. Appl. Biochem. 46 (2007) 73–84.
[15] S. Bae, Y. Sugano, M. Shoda, J. Biosci. Bioeng. 97 (2004) 33–38.
[16] T. Ishida, M. Mitarai, Y. Sugano, M. Shoda, Biotechnol. Bioeng. 83 (2003) 474–478.
[17] M. Seifert, S. Hesse, V. Kabrelian, D. Klemm, J. Polym. Sci., Part A: Polym. Chem. 42 (2003) 463–470.
[18] A. Hirai, M. Tsuji, H. Yamamoto, F. Horii, Cellulose 5 (1998) 201–213.
[19] Z. Yan, S. Chen, H. Wang, B. Wang, C. Wang, J. Jiang, Carbohydr. Res. 343 (2008) 73–80.
[20] G. Joseph, G.E. Rowe, A. Margaritis, W. Wan, J. Chem. Technol. Biotechnol. 78 (2003) 964–970.
[21] P.J. Weimer, J.M. Hackney, H.J. Jung, R.D. Hatfield, J. Agric. Food Chem. 48 (2000) 1727–1733.
[22] S.E.C. Whitney, J.E. Brigham, A.H. Darke, J.S.G. Reid, M. Gidley, Plant J. 8 (1995) 491–504.
[23] C. Tokoh, K. Takabe, M. Fujita, H. Saiki, Cellulose 5 (1998) 249–261.
[24] S. Keshk, Enzyme Microb. Technol. 40 (2006) 9–12.
[25] K.C. Cheng, M.J. Catchmark, A. Demirci, Cellulose 16 (2009) 1033–1045.
[26] R. Mendichi, A.G. Schieroni, Polymer 43 (2002) 6115–6121.
[27] B. Widner, R. Behr, S. Von Dollen, M. Tang, T. Heu, A. Sloma, D. Sternberg, P.L. De Angelis, P.H. Weigel, S. Brown, Appl. Environ. Microbiol. 71 (2005) 3747–3752.
[28] R.N. Rosier, R.J. O'Keefe, Instr. Course Lect. 49 (2000) 495–502.
[29] M.B. Brown, S.A. Jones, J. Eur. Acad. Dermatol. Venereol. 19 (2005) 308–318.
[30] K.S. Girish, K. Kemparaju, Life Sci. 80 (2007) 1921–1943.
[31] A. Sannino, M. Madaghiele, F. Conversano, G. Mele, A. Maffezzoli, P.A. Netti, L. Ambrosio, L. Nicolais, Biomacromolecules 5 (2004) 92–96.
[32] A. Sannino, S. Pappadà, M. Madaghiele, A. Maffezzoli, L. Ambrosio, L. Nicolais, Polymer 46 (2005) 11206–11212.
[33] S. Hestrin, M. Schramm, J. Biochem. 58 (1954) 345–352.
[34] L. Segal, J.J. Creely, A.E. Martin, C.M. Conrad, Text. Res. J. 29 (1959) 786–794.
[35] User's Guide - Agilent Technologies 5500 Scannng Probe Microscope, Edition Rev B-6, October, 2009: Palo Alto, CA.
[36] D.Y. Kwok, A.W. Neumann, Adv. Colloid Interface Sci. 81 (1999) 167–249.
[37] J. Sugiyama, J. Persson, H. Chanzy, Macromolecules 24 (1991) 2461–2466.
[38] Y. Marechal, H. Chanzy, J. Mol. Struct. 523 (2000) 183–196.
[39] H. Yamamoto, F. Horii, A. Hirai, Cellulose 3 (1996) 229–242.
[40] R. Gilli, M. Kacurakova, M. Mathlouthi, L. Navarini, S. Paoletti, Carbohydr. Res. 263 (1994) 315–326.
[41] W. Yue, Carbohydr. Polym. 89 (2012) 709–712.
[42] K. Haxaire, Y. Maréchal, M. Milas, M. Rinaudo, Biopolymers 72 (2003) 10–20.
[43] M.N. Collins, C. Birkinshaw, Carbohydr. Polym. 92 (2013) 1262–1279.
[44] J.R. Glass, K.T. Dickerson, K. Stecker, J.W. Polarek, Biomaterials 17 (1996) 1101–1108.
[45] U. Hersel, C. Dahmen, H. Kessler, Biomaterials 24 (2003) 4385–4415.
[46] M.D. Pierschbacher, E. Ruoslahti, Nature 309 (1984) 30–33.
[47] T. Asakura, H. Nishi, A. Nagano, A. Yoshida, Y. Nakazawa, M. Kamiya, M. Demura, Biomacromolecules 12 (2011) 3910–3916.
[48] E.M. Harnett, J. Alderman, T. Wood, Colloids Surf., B: Biointerfaces 55 (2007) 90–97.
[49] M. Benziman, C.H. Haigler, R.M. Brown Jr., A.R. White, K.M. Cooper, Proc. Nat. Acad. Sci. U.S.A. 77 (1980) 6678–6682.
[50] A.C. O'Sullivan, Cellulose 4 (1997) 173–207.
[51] Y. Nishiyama, J. Wood Sci. 55 (2009) 241–249.
[52] H. Yamamoto, F. Horii, Cellulose 1 (1994) 57–66.
[53] L.L. Zhou, D.P. Sun, L.Y. Hu, Y.W. Li, J.Z. Yang, J. Ind. Microbiol. Biotechnol. 34 (2007) 483–489.
[54] S.E.C. Whitney, J.E. Brigham, A.H. Darke, J.S.G. Reid, M.J. Gidley, Plant J. 8 (1995) 491–504.
[55] S.K. Cousins, R.M. Brown Jr., Polymer 36 (1995) 3885–3888.
[56] I. Bravo-Osuna, M. Noiray, E. Briand, A.M. Woodward, P. Argüeso, I.T.M. Martínez, R. Herrero-Vanrell, G. Ponchel, Pharm. Res. 29 (2012) 2329–2340.
[57] Y. Tamada, Y. Ikada, J. Biomed. Mater. Res. 28 (1994) 783–789.
[58] J.M. Goddard, J.H. Hotchkiss, Prog. Polym. Sci. 32 (2007) 698–725.
[59] L.C. Xu, Biomaterials 28 (2007) 3273–3283.
[60] S. Gerecht, J. Burdick, L. Ferreira, S. Townsend, R. Langer, G. Vunjak-Novakovic, Proc. Nat. Acad. Sci. U.S.A. 104 (2007) 11298–11303.